

Assessment and Validation of $\cos\alpha$ Method for Residual Stress Measurement

Nate Peterson ^a, Yuji Kobayashi ^b, Bill Traeger ^c, Paul Sanders ^a

^a Michigan Technological University, USA, nepeters@mtu.edu, sanders@mtu.edu;

^b SINTOKOGIO CO. LTD., Japan, y-kobayashi@sinto.co.jp

^c SINTO AMERICA, USA, bill.traeger@robertssinto.com

Keywords: residual stress, x-ray diffraction, experimental methods

Abstract

For proper control of shot peening surface treatments, measurement of residual stresses in the treated material is an important consideration. Traditionally, X-ray diffraction techniques have allowed for non-destructive testing of the material for qualification purposes by utilizing traditional stationary diffractometers. Recently, portable residuals stress analyzers have seen increased interest due to the ease of use. The $\cos\alpha$ technique has shown promise as a faster method of measuring residual stresses in portable devices due to its ability to measure an entire Debye ring at once from the two-dimensional detector, thus not requiring multiple sample tilts. In this study, shot-peened and in-situ loaded steel samples were subjected to residual stress measurement from both the $\cos\alpha$ and $\sin^2\psi$ technique using a portable device and laboratory diffractometer respectively. Two types of data analyses were performed to calculate the residual stresses based on linear-regression and least-squares analysis. The results from this work show the equivalency in both accuracy and precision of the $\cos\alpha$ to the traditional $\sin^2\psi$ technique in measuring residual stresses in shot-peened materials. Based on these results, recommendations are presented on the use of x-ray diffraction for residual stress measurement.

Introduction

In mechanical design, residual stresses are a crucial factor in avoiding failure due to fatigue crack nucleation and propagation. A variety of methods, such as shot peening, are employed to create a compressive residual stress field to limit crack nucleation in critical parts.¹⁻³ An adequate method of measuring the stress fields present in these materials after processing is crucial for verification and understanding the mechanical behavior. Destructive and non-destructive methods; such as sectioning/hole drilling and x-ray diffraction, are used to measure residual stresses. A common x-ray diffraction method, the $\sin^2\psi$ method, is time intensive and requires a full X-ray diffractometer setup with a proper goniometer for measurement. The $\cos\alpha$ technique has shown promise as a faster evaluation technique with similar errors when compared to the $\sin^2\psi$ technique.^{4,5} Portable x-ray stress analyzers have been under development since the late 1970s, utilizing position-sensitive detectors in order to calculate the stress via the $\sin^2\psi$ method with the single exposure technique highlighted by James et al.⁶ Recent development has focused on advanced image plate 2-dimensional detectors to replace film for portable detectors, particularly with XRD² by He et al.⁷ and the $\cos\alpha$ by Sasaki et al. With advancements in miniaturization of other x-ray diffraction components (sources, optics, control electronics, etc.) the creation of portable two-dimensional x-ray diffractometers for portable residual stress measurement was made possible. Although development has rapidly increased in the past decade, agreement on the equivalency of the $\sin^2\psi$, $\cos\alpha$ and other 2D techniques is still up for debate. Very little work has compared the uncertainties from the $\cos\alpha$ and $\sin^2\psi$ techniques.^{8,9} This work will directly compare the $\sin^2\psi$ method using a traditional diffractometer and the $\cos\alpha$ methods using a portable device to objectively assess measurement capability.

Background

X-ray diffraction measurements

As with any x-ray diffraction based technique, factors such as; grain size, preferred orientations, diffracting volume, and geometric alignment must be considered with assessing the results. When measuring residual stress, the assumption can be made that the sample has a homogenous stress field present, therefore variations on the diffracting volume from sample tilts should not significantly change the stress field being measured. While this is a strong assumption to make, it has been shown that for shot-peened materials the random plastic deformation induced by the peening eliminates the effects of preferred orientation and heterogeneous stress fields,¹⁰ therefore for the shot-peened samples in this work an isotropic stress field is assumed. However, in uniaxial tension or compression these factors should be considered and each sample should be checked to make sure there isn't any preferred orientation. In samples in which a preferred orientation has occurred, a phenomenon known as pseudo-macrostress can occur which can give erroneous results if not accounted for. This has been explored by Cohen and others¹⁰⁻¹³ in previous works.

Stress measurement via $\sin^2\psi$ method

Traditional x-ray diffraction-based residual stress measurement methods have utilized the $\sin^2\psi$ method with either a θ/θ or $\theta/2\theta$ goniometer setup.^{5,14}

The measurement relies on the ability to measure the fundamental atomic plane spacing, d_0 , and the change in d as a result of processing. This measured lattice spacing is expressed as the $d_{\psi\phi}$ relating this measured lattice spacing at the various diffractometer angles, ψ and ϕ (Figure 1).¹⁴ This translation from the diffractometer space to the sample space is fundamental to the derivation of both the $\sin^2\psi$ and $\cos\alpha$ methods. By relating this measured lattice spacing to the strain components in the sample space, the measured lattice spacing may be represented from the diffraction vector \mathbf{n} , through Einstein notation as $\varepsilon_{\phi\psi} = n_i n_j \varepsilon_{ij}$. This strain can be inserted into Hooke's law to yield equation (3).

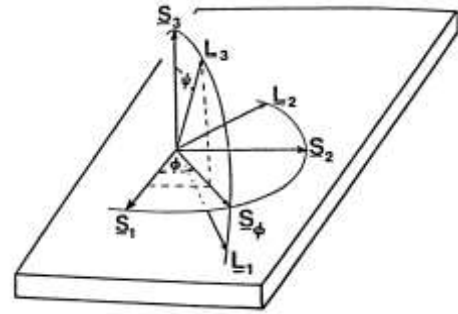


Figure 1: Depiction of the laboratory coordinate system and sample coordinate system with the ϕ and ψ angles used for translation from the diffraction vector and sample coordinates.

$$\mathbf{n} = \begin{bmatrix} \sin \psi \cos \phi \\ \sin \psi \sin \phi \\ \cos \psi \end{bmatrix} \quad (1)$$

$$\varepsilon_n = n_1^2 \varepsilon_{11} + n_2^2 \varepsilon_{22} + n_3^2 \varepsilon_{33} + 2n_1 n_2 \varepsilon_{12} + 2n_1 n_3 \varepsilon_{13} + 2n_2 n_3 \varepsilon_{23} \quad (2)$$

$$\varepsilon_{\phi\psi} = \frac{d_{\phi\psi} - d_0}{d_0} = \frac{1+\nu}{E} (\sigma_{11} \cos^2 \phi + \sigma_{12} \sin 2\phi + \sigma_{22} \sin^2 \phi) \sin^2 \psi - \frac{\nu}{E} (\sigma_{11} + \sigma_{22}) \quad (3)$$

Equation (3) is commonly used as the fundamental equation for the $\sin^2\psi$ analysis method. \

Stress measurement via $\cos \alpha$ method

The $\cos\alpha$ method utilizes the Debye ring collected with a single measurement using a 2D detector (Figure 2), as described by Sasaki et al.⁴ and others.⁸ The translation from the diffractometer space to the sample space is inherently more complex due to the 2D planar geometry of the measurement and can be represented as

$$\mathbf{n} = \begin{bmatrix} \cos \eta \sin \psi_o + \sin \eta \cos \psi_o \cos \alpha \\ \cos \eta \sin \psi_o \sin \phi_o + \sin \eta \cos \psi_o \sin \phi_o \cos \alpha + \sin \eta \cos \phi_o \sin \alpha \\ \cos \eta \cos \psi_o - \sin \eta \sin \psi_o \cos \alpha \end{bmatrix} \quad (4)$$

form of the expression for the translation of strain, $\varepsilon_\alpha = n_i n_j \varepsilon_{ij}$, which can be inserted into Hooke's law to form

$$\varepsilon_\alpha = \frac{1+\nu}{E} n_i n_j \varepsilon_{ij} - \frac{\nu}{E} \sigma_{kk} \quad (5)$$

Defining two parameters, a_1 and a_2 allows for linear determination of both σ_{11} and σ_{22} if both a ϕ_o and ψ_o have been chosen and kept constant for the data collection.

$$a_1 = \frac{1}{2} [(\varepsilon_\alpha - \varepsilon_{\pi+\alpha}) + (\varepsilon_{-\alpha} - \varepsilon_{\pi-\alpha})] \quad (6)$$

$$a_2 = \frac{1}{2} [(\varepsilon_\alpha - \varepsilon_{\pi+\alpha}) - (\varepsilon_{-\alpha} - \varepsilon_{\pi-\alpha})] \quad (7)$$

$$a_1 = \frac{1+\nu}{E} \sigma_{11} \sin 2\psi_o \sin 2\eta \cos \alpha \quad (8)$$

$$a_2 = 2 \frac{1+\nu}{E} \sigma_{12} \sin \psi_o \sin 2\eta \sin \alpha \quad (9)$$

Thus, the term $\cos \alpha$ in the a_1 term is the origin of the name for the method. Since each point measured by the device depends only on the Debye ring coordinates and sample orientation (ψ_o , ϕ_o , α , η), equation (5) may also be solved for via a least-squares analysis, which can lead to improved accuracy in the stress measurement. For more in-depth analysis of biaxial and triaxial stress states, generally two or more ψ_o tilts are required.

Least-squares analysis of $\sin^2 \psi$ and $\cos \alpha$ measurement methods

Initial work done with residual stress measurement dealt with linear-regression methods of solving for stress values, due to simplicity and speed of analysis. Recent advances have shown that using a generalized least-squares approach to solve for the stress values have been shown to reduce the errors associated with the measurement. For this work, both linear-regression and least-squares methods will be employed to fully understand the errors associated with each method. This generalized least-squares method was first outlined in Miyazaki and Sasaki⁵ and Winholtz and Cohen¹⁵, but will be described in brief here. For any set of k diffraction vectors, a set of \mathbf{n} vectors can be defined and used to create a $k \times 6$ matrix,

$$F \equiv \begin{bmatrix} n_{11}^2 & n_{12}^2 & n_{13}^2 & 2n_{11}n_{12} & 2n_{11}n_{13} & 2n_{12}n_{13} \\ \vdots & \vdots & \vdots & \vdots & \vdots & \vdots \\ n_{k1}^2 & n_{k2}^2 & n_{k3}^2 & 2n_{k1}n_{k2} & 2n_{k1}n_{k3} & 2n_{k2}n_{k3} \end{bmatrix} \quad (10)$$

Then this F matrix can be used with the fundamental equation (2) to solve for the strains in the sample space,

$$\varepsilon_n = F [\varepsilon_{ij}] \quad (11)$$

This equation for the strains in the sample space can then be utilized in a conversion to stresses following Hooke's law, $\varepsilon_{ij} = C_{ijkl} \sigma_{kl}$ thus resulting in the equation below, which is the Moore-Penrose general inverse of M . The standard deviation of any given stress value is given by equation (13).

$$\varepsilon_n = F * S \sigma = M \sigma \rightarrow \sigma_n = \mathbf{M}^+ \varepsilon_n \quad (12)$$

Where \mathbf{n} can be used in

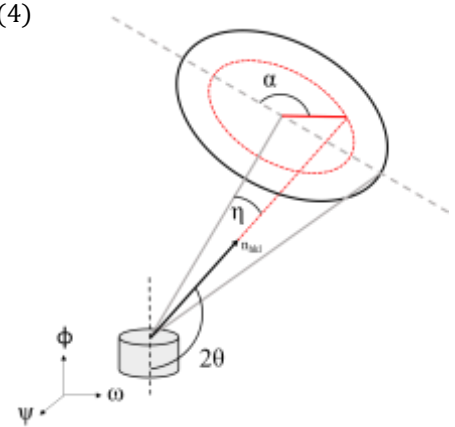


Figure 2: Geometric representation of the $\cos(\alpha)$ geometry using a two-dimensional detector. The sample space axes (ϕ , ψ , ω) are shown in the bottom left, along with the critical α , η , and 2θ angles on the Debye ring.

$$s_{\sigma_{ij}} = s_{\varepsilon_{\alpha}} \sqrt{\sum_{i=1}^k (M_{ij}^+)^2} \quad (13)$$

Methodology

In this work two separate devices were used to collect diffraction data from both standard shot-peened samples and in-situ during uniaxial tension, a Scintag XDS2000 diffractometer with Pole-Texture-Stress (PTS) goniometer and a Sinto PSMX-I portable residual stress analyzer. For the $\sin^2\psi$ data collection, the Scintag XDS2000 PTS was used with a Cr tube with a 1mm point collimator on the incident beam and 1 and 0.5mm fixed slits on the diffracted beam. The scans were run at 45kV and 30mA with a step size of 0.02° 2θ and a count time of 15sec per step using the Scintag DMSNT software package. The PSMX-I device contains a Cr tube with a 1mm point collimator on the incident beam with a back-reflection mounted two-dimensional detector. The image plate detector has a spatial resolution of $50\mu\text{m}$, which was used at working distances of 37 for the standard shot-peened samples and 39mm for in-situ tests at a ψ_0 angle of 35° for all testing. The device has an x-ray exposure time of approximately 30 seconds with an overall measurement time of 90 seconds.



Figure 3: Photo of proof ring-based load cell used to apply a tensile load in-situ during the x-ray diffraction experiments. The same load cell was used with both the $\sin^2\psi$ and $\cos\alpha$ measurement methods.

For the in-situ loading tests, a small circular proof ring based load cell^{16,17} was created to test the same sample under load for both methods (Figure 3). The ring used in this work had an outer diameter of 14cm, inner diameter of 13cm and a width (b) of 2.54cm. The load cell was calibrated using four strain gauges set up in a Wheatstone bridge configuration. The tensile sample used was a AISI 1045 steel bar that was annealed in a vacuum furnace prior to testing to remove any prior residual stresses present in the material. Optical microscopy confirmed no preferred orientation was present in the tensile load sample, and no preferred orientation was assumed for the shot-peened samples. The tensile bar was custom made with a gauge length of 37mm and a gauge thickness of 4mm. Five scans with each method were run at a 50, 100 and 150MPa applied tensile load along with the -400, -800 and -1600MPa shot-peened (compressive load) standard samples. Each data set collected were used to calculate the residual stresses using both the linear-regression and least-squares options. The elastic constants ($E=224\text{GPa}$ and $\nu=0.28$) were used for both the linear-regression and generalized least-squares options for calculating the stress from the experimental data.

Results and analysis

Measurement results show that the $\sin^2\psi$ and $\cos\alpha$ methods produce comparable results with standardized samples and the in-situ loaded samples (Table 1). These results were calculated using the traditional line fitting method of $\sin^2\psi$ vs d and $\cos\alpha$ vs a_1 respectively. Figure 4 shows a plot of the $\sin^2\psi$ vs $\cos\alpha$ methods respectively with each analysis option, showing a linear trend with very little variance between the two methods at each stress level. These results show the accuracy is virtually equivalent for each method, showing the feasibility of using the two-dimensional detector type of portable residual stress analyzers in critical applications. It was also found that the ψ_0 tilt angle was a major source of alignment errors with the $\cos\alpha$ method (Figure 5). Due to the nature of the two-dimensional detector and portable device proper alignment is more critical due to the wider

range of the diffraction condition window, whereas on a fixed goniometer setup ($\sin^2\psi$), the diffraction condition window is much tighter, thus proper alignment is necessary before any signal will even be seen by the detector.

Recently published results also agree with the data found in this experiment; Lee et al. conducted an extensive investigation into the accuracy and precision of the two-dimensional detector $\cos\alpha$ and found that two methods agree, however properly setting ψ_0 tilt angle is crucial for accurate measurements and that consideration must be taken for assumptions about preferred orientation in the material. ⁹ These factors are important to understand to achieve proper measurement results from these methods. It is

strongly recommended that every unique material and processing schedule be verified before these assumptions are made. Critical attention should also be paid to sample alignment and the x-ray elastic constants used as those make up most of the errors associated with these techniques. The data calculated using the generalized least-squares option suggests that further calibration of the x-ray elastic constants may be necessary to achieve accurate results. The standard deviation of the calculated stress values is significantly increased when using the generalized least-squares option, as it accounts for all the measured diffraction vectors, \mathbf{n}_i in the analysis. The error is proportional to the square of the number of vectors used in the analysis, as shown with equation (13) While the generalized least-squares analysis does provide more precise calculation of the stress values from a given diffraction measurement, it does require extra computational power that can increase the total time of analysis. Another distinction between the linear-regression and generalized least-squares options for the $\cos\alpha$ measurement method is the averaging of strains across the Debye ring for the linear-regression (equations 6 & 7), which could be a source of the increased uncertainty in the resulting calculation. Overall, the $\cos\alpha$ and $\sin^2\psi$ methods agree in the calculated results, with similar precision and accuracy for a chose data analysis option.

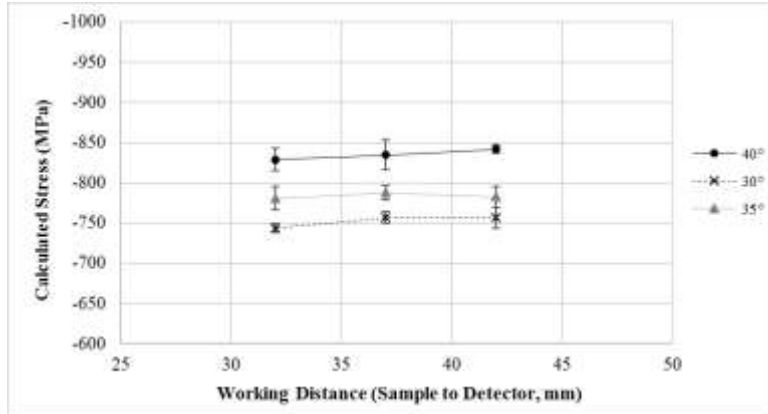


Figure 5: Plot of the calculated stress level ($\cos\alpha$ method) in the -800MPa shot peened sample as a function of working distance, with each ψ_0 angle tested; 40, 35 and 30°. The error bars show one standard deviation for each measurement.

Table 1: Averaged collected data from both the $\sin^2\psi$ method and $\cos\alpha$ method along with standard deviations derived from the stress calculation method of linear-regression. – needs to be updated with data from least-squares

Sample	$\sin^2\psi$ Method Measured Stress				$\cos\alpha$ Method Measured Stress			
	Linear Regression	$\pm 1\sigma$	Least Squares	$\pm 1\sigma$	Linear Regression	$\pm 1\sigma$	Least Squares	$\pm 1\sigma$
-1600MPa	-1594	49	-1399	6	-1625	37	-1402	2
-800MPa	-760	36	-806	5	-796	14	-810	1
-400MPa	-388	5	-307	3	-396	6	-311	1
0MPa	0	4	-13	1	0	2	-19	1
50MPa	49	6	46.2	1	49	5	36	1
150MPa	146	5	139.0	2	148	4	142	1

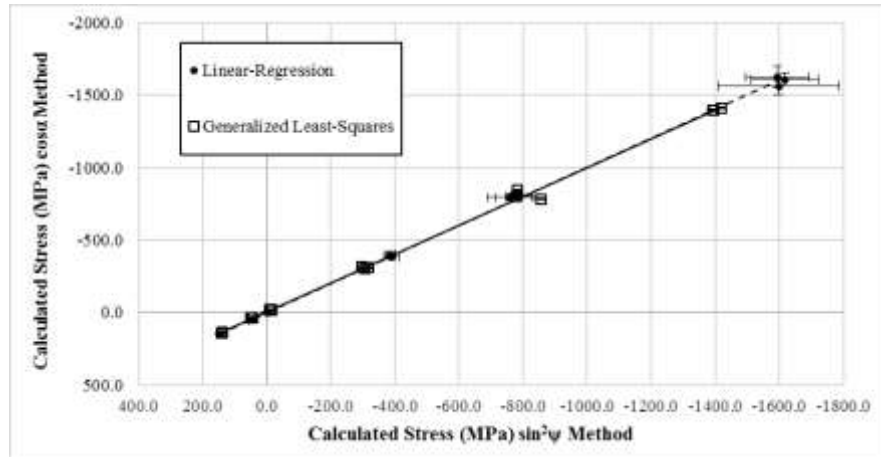


Figure 4: Plot of calculated stress values from $\sin^2\psi$ and $\cos\alpha$ and for each stress level comparing the two measurement methods and analysis options. Error bars represent two standard deviations.

Conclusions

In shot-peening process control, knowledge of the residual stresses before and after processing can be a principal factor in producing quality material for intended service conditions. The advent of new techniques for measuring these residual stresses, such as the $\cos\alpha$ technique, was found to provide rapid residual stress measurement with comparable results to traditional methods. However, some precautions must be taken to properly achieve accurate and precise results.

1. Careful consideration to the processing history and structure of the material, as preferred orientation can result in erroneous results.
2. Alignment errors can be a large issue on the $\cos\alpha$ device, particularly with the ψ_0 tilt angle. The $\sin^2\psi$ method using a laboratory diffractometer is less susceptible to these errors due to the fixed geometry, however this all but inhibits portability.
3. The generalized least-squares approach shows promise as a more precise data analysis option for both the $\sin^2\psi$ and $\cos\alpha$ methods.

References

1. Benedetti, M., Fontanari, V., Höhn, B.-R., Oster, P. & Tobie, T. Influence of shot peening on bending tooth fatigue limit of case hardened gears. *Int. J. Fatigue* **24**, 1127–1136 (2002).
2. Torres, M. & Voorwald, H. An evaluation of shot peening, residual stress and stress relaxation on the fatigue life of AISI 4340 steel. *Int. J. Fatigue* **24**, 877–886 (2002).
3. Cammet, J. Quality assurance of shot peening by automated surface and subsurface residual stress measurement. *Shot Peen.* **15**, 7–8 (2001).
4. Sasaki, T. New Generation X-Ray Stress Measurement Using Debye Ring Image Data by Two-Dimensional Detection. *Mater. Sci. Forum* **783–786**, 2103–2108 (2014).
5. Miyazaki, T. & Sasaki, T. A comparison of X-ray stress measurement methods based on the fundamental equation. *J. Appl. Crystallogr.* **49**, (2016).
6. James, M. & Cohen, J. B. 'PARS'—A Portable X-Ray Analyzer for Residual Stresses. *J. Test. Eval.* **6**, 91–97 (1978).
7. He, B. B., Preckwinkel, U. & Smith, K. L. Fundamentals of two-dimensional X-ray diffraction (XRD2). *Adv X-Ray Anal* **43**, 273–80 (2000).

8. Ramirez-Rico, J., Lee, S.-Y., Ling, J. J. & Noyan, I. C. Stress measurement using area detectors: a theoretical and experimental comparison of different methods in ferritic steel using a portable X-ray apparatus. *J. Mater. Sci.* **51**, 5343–5355 (2016).
9. Lee, S.-Y., Ling, J., Wang, S. & Ramirez-Rico, J. Precision and accuracy of stress measurement with a portable X-ray machine using an area detector. *J. Appl. Crystallogr.* **50**, 131–144 (2017).
10. Cullity, B. D. Some problems in X-ray stress measurements. in *Proc. Conf. on Advances in X-Ray Analysis, 1977, 20, 259-271* (1977).
11. James, M. R. & Cohen, J. B. *Study of the Precision of X-Ray Stress Analysis*. (DTIC Document, 1976).
12. Hauk, V. & Vaessen, G. X-Ray Stress Analysis of Textured Steels. *Intern. Stress Orig.-Meas.--Eval. Eig. Entsteh.--Mess.--Bewert. Vol 2 Karlsr. FRG 14-15 Apr 1983* 9–30 (1983).
13. Haase, A., Klatt, M., Schafmeister, A., Stabenow, R. & Ortner, B. The generalized sin² [psi] method: An advanced solution for X-ray stress analysis in textured materials. *Powder Diffr.* **29**, 133–136 (2014).
14. Noyan, I. C. & Cohen, J. B. *Residual Stress: Measurement by Diffraction and Interpretation*. (Springer, 2013).
15. Winholtz, R. A. & Cohen, J. B. Generalised least-squares determination of triaxial stress states by x-ray diffraction and the associated errors. *Aust. J. Phys.* **41**, 189–200 (1988).
16. Bray, A. The role of stress analysis in the design of force-standard transducers. *Exp. Mech.* **21**, 1–20 (1981).
17. Kumar, H., Sharma, C. & Kumar, A. Design and development of precision force transducers. (2011).